# Chapter 5

*Biosensor fabrication by immobilizing GST enzyme on platinum electrode using graphene oxide mediator*

## 5.1 Introduction

Enzyme immobilization appears as a crucial factor to develop efficient biosensors with appropriate performances such as high reproducibility, high selectivity, high sensitivity, short response time, good operational and storage stability etc. Immobilization significantly improves the stability of the biomolecules under various reaction conditions and enhances the reusability of biomolecules over successive catalytic cycles. Moreover, immobilization renders the biocatalysts to change from a homogeneous to a heterogeneous form, which facilitates simple separation of the biocatalytic system from the reaction mixture and results in products of higher purity [1]. Immobilization matrix plays a key role in the functioning of biosensors. Different immobilization matrices have been used for immobilization of enzymes such as conducting polymers [2,3], carbon nanotubes [4,5], graphene oxide [6,7], silica sol-gel [8,9] and clay material [10] etc.

Considering the extremely small size and the excellent performance in immobilizing enzymes, nanoparticles can act as favourable choice for enzyme immobilization. However, the following two major problems need to be addressed firstly: (1) the non-coagulation of immobilized enzyme by the used matrix; and (2) a high loading capacity for enzyme. Carbon-based nanomaterials, such as graphene has attracted considerable interest among the nanostructured materials, which could provide a good opportunity to resolve these problems [11]. Graphene together with its various derivatives, such as graphene oxide, graphene nanoribbon, chemically reduced graphene oxide, or nitrogen doped graphene, has shown captivating properties to use in electrochemistry such as electrochemical devices, capacitors or transistors [12-14].

Graphene, a kind of nanomaterial with a monolayer of $sp^2$ hybridized carbon atoms, has driven increasing research interests due to its remarkable properties, such as extremely high thermal conductivity, high mobility of charge carriers, high surface area-to-volume ratio and good biocompatibility. The unique properties of graphene give it potential applicability in electrochemical biosensors [15]. Graphene oxide (GO), as a basic material for the preparation of individual graphene sheets in bulk-quantity, has especially attracted increasing research interests due to its remarkable properties, such as incredibly large specific surface area (two accessible sides), the abundant oxygen containing

surface functionalities, such as epoxide, hydroxyl, and carboxylic groups, and the high water solubility afford GO sheets great promise for biosensor applications [16].

In this chapter we have shown fabrication of biosensor probes through immobilization of GST in graphene oxide which can be used for detection of wide varieties of pesticide classes. To our knowledge this is for the first time that the enzyme GST has been immobilized using graphene oxide matrix for electrochemical biosensor application. Gelatin (Gel) has been used as binder for binding the enzyme molecules on GO supported matrix. It is a linear polypeptide with excellent membrane forming ability, biocompatibility and nontoxicity. It facilitates natural microenvironment to the enzyme and also provides sufficient accessibility to electrons to shuttle between the enzyme and the electrode [15]. Finally, GST was entrapped in GO-Gel matrix through glutaraldehyde (Glut) cross-linking to improve the stability of the biosensor. Without cross-linking, the biosensor does not exhibit sharp step-like response and the current signal is small [17].

Advantages of the immobilized GST biosensor over the free enzyme technique is obvious from the facts that 1. it is reusable for 8-10 consecutive measurements thus offering cost efficiency and 2. it can be used in chronoamperometric mode, thus showing the feasibility of real time monitoring application. The biosensor can be applied to detect a broad spectrum of pesticides covering at least six different classes namely- benzimidazole, organochlorine, organothiophosphate, organocarbamate, polyphenol and pyrethroid. Application to pyrethroids, organocarbamates and organothiophosphate were demonstrated in previous chapters [18,19] while the application to the remaining classes have been done in the present chapter.

## 5.2 Objectives of this chapter

- Fabrication of biosensor probe through immobilization of GST in a GO matrix.
- GST will be immobilized through entrapment on GO-gelatin matrix. Cross linker gluteraldehyde be used to prevent enzyme leaching.
- Immobilization will be confirmed through SEM and electrochemical study.
- Electrochemical behavior of GO-Gel-GST-Glut modified electrode will be studied.

- Optimization of operational conditions for maximum signal output will be done by evaluating the saturated substrate concentration, maximum enzyme loading and optimum pH.
- Basic enzyme kinetic parameters relevant to the GST catalyzed GSH-CDNB reaction will be evaluated.
- Suitable reactivation mechanism will be worked out for reuse of the sensor.
- Application of the sensor to analyze test samples of different classes of pesticides such as benzimidazole (carbendazim), organochlorine (DDT), organothiophosphate (ethion and chlopyrifos) and polyphenol (dinocap).
- Validation study to be carried out using GC/GC-MS.

## 5.3 Experimental

### 5.3.1 Synthesis of graphene oxide

Graphene oxide (GO) was synthesized using modified Hummers' method [20]. In brief, graphite powder (0.5 g) and $NaNO_3$ (0.5 g) were mixed in 23 mL of $H_2SO_4$ (98%) in a conical flask kept under ice bath (0-5 $^0$C) with continuous stirring. The mixture was stirred for 4 hrs at this temperature and then potassium permanganate (3 g) was added to the mixture very slowly. The rate of addition was carefully controlled keeping the mixture in ice bath. This mixture was stirred for 1 hr and then ice bath was removed. Next, heated the mixture at 35 $^0$C and stirred for another 1 hr. The mixture was diluted with very slow addition of 46 mL water under stirring which led to increase of temperature up to 95 $^0$C. This temperature was maintained for 2 hrs. Then the heater was turned off and allowed the mixture to cool at room temperature and added 100 mL distilled water under stirring for next 1 hr. The solution was finally treated with 10 mL of 30% $H_2O_2$ by which the color got changed to bright yellow. Then it was allowed to stay for 3-4 hrs, whereby the particles settled at the bottom and the remaining water was poured to filter. The resulting mixture was washed repeatedly by centrifugation with 5% HCl and then with deionized (DI) water several times until it forms gel like substance (pH- neutral). After centrifugation, the gel like substance was vacuum dried at 60 $^0$C for more than 6 hrs to get GO powder.

### 5.3.2 Biosensor preparation

Prior to use, platinum working electrode was first polished on aqueous slurries of 1 μM, 0.3 μM and 0.05 μM alumina powder. After thorough rinsing in deionized water followed by acetone, the electrode was dipped for about 5 minutes in a hot 'Piranha' solution (1:3 (v/v) 30 % $H_2O_2$ and concentrated $H_2SO_4$) and rinsed again with copious amounts of deionized water. 5% gelatin solution was prepared by warming gelatin water mixture up to 60 $^0$C followed by cooling down to room temperature. 2.0 mg GO was added to 1.0 mL of gelatin aqueous solution to form homogenous dispersion with sonication. The modified electrode was prepared by a simple drop casting method as follows: initially, the pretreated Pt was modified by dropping 20 μL of the GO/gelatin solution keeping the electrode vertical and allowed to be dried in ambient air for 1 hr to obtain GO/GEL/Pt modified electrode; then the obtained electrode was coated with 20 μL GST solutions, which was incubated for another 2 hrs; after that 20 μL of glutaraldehyde (35% in water) was added to the electrode tip with a micro syringe. The electrode was then kept at room temperature in the same vertical position until the film appeared dry (for approximately 4 hrs). The prepared sensor was stored at 4 $^0$C when not in use.

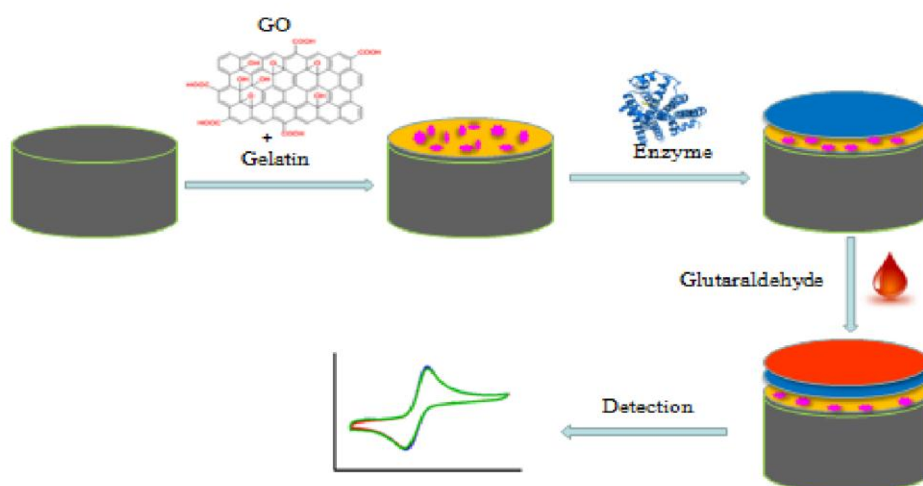


Scheme 5.1. Schematic representation of biosensor preparation.

### 5.3.3 Analytical procedure

#### 5.3.3.1 Electrochemical measurements

Cyclic Voltammetric (CV) measurements were done in the potential range from − 0.4 V to 1 V, at scan rate 20 mV/s. Chronoamperometric (CA) analysis was done setting the parameters as $E_0 = 0.0$ V applied for 30 s, $E_1 = 0.30$ V applied for 100 s.

Cleaning of all electrodes was done before each experiment. Pt electrode was cleaned by polishing in γ-$Al_2O_3$ (0.05 μM) until a shining surface was obtained and sonicated for 5-10 minutes using digital ultrasonic cleaner. Electrodes were then dipped in PB and cycled from -1.0 to +1.0 V until it acquired at a steady state baseline. Prior to electrochemical measurement the solution mixtures were mixed thoroughly and then the measurements were made in static solution condition. The total volume of the working solution in the electrochemical cell was 3 mL and prepared by mixing 1.5 mL of 2 mM GSH in PB with 1.5 mL of 2 mM CDNB in 50% methanol, unless stated otherwise.

#### 5.3.3.2 Gas chromatographic measurements

A gas chromatogram with auto injector system was used for pesticide analysis. Ultra pure helium was used as the carrier gas at constant flow rate of 1.0 mL/min. The injector and detector temperatures were set at 250 $^0$C. The oven temperature was programmed as follows: initial 80 $^0$C was hold for 5 min and then programmed from 80 to 250 $^0$C at 15 $^0$C/min and hold for 20 min. The total time for one GC run was 36 min and injected volume was 1 μL each time through auto-injection mode.

## 5.4 Results and Discussion

### 5.4.1 Characterization

X-ray diffraction spectra (Figure 5.1) of GO showed peak at 2θ = 10.36 $^0$ which is very close to the reported XRD pattern of GO corresponding to (001) crystal plane. FTIR spectrum shows (Figure 5.2) the presence of O-H stretching vibrations (3429 $cm^{-1}$), C=O stretching vibration (1728 $cm^{-1}$), C=C from unoxidized $sp^2$ C-C bonds (1626 $cm^{-1}$), and C-O vibrations (1053 $cm^{-1}$) which are characteristic peaks of GO as per literature [21].

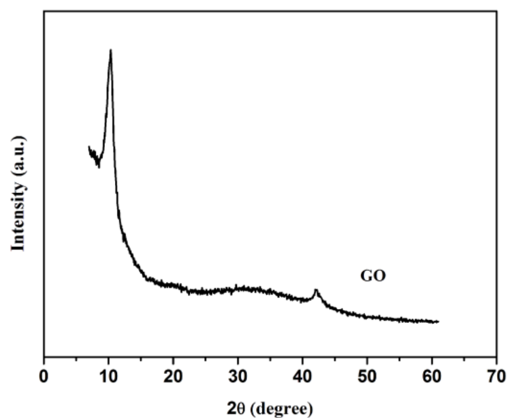


Figure 5.1. XRD pattern of synthesized GO.

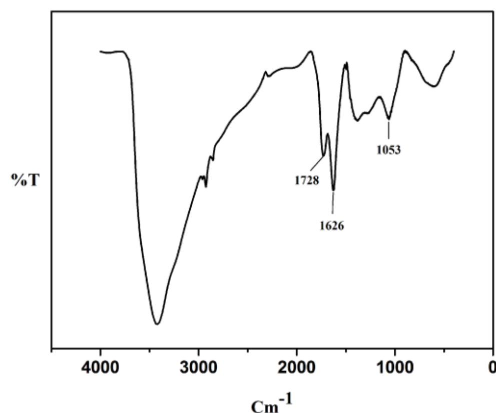


Figure 5.2. IR spectrum of GO.

Morphology of the fabricated electrode was studied by SEM analysis. SEM images of GO, gelatin-gluteraldehyde mixed GO (GO/Gel/Glut) and GST immobilized graphene oxide-gelatin-glutaraldehyde composite (GO/Gel/GST/Glut) films are shown in Figure 5.3. SEM images clearly show the flake type morphology of GO (Figure 5.3a) and the well dispersed thread shaped enzyme units (Figure 5.3c).

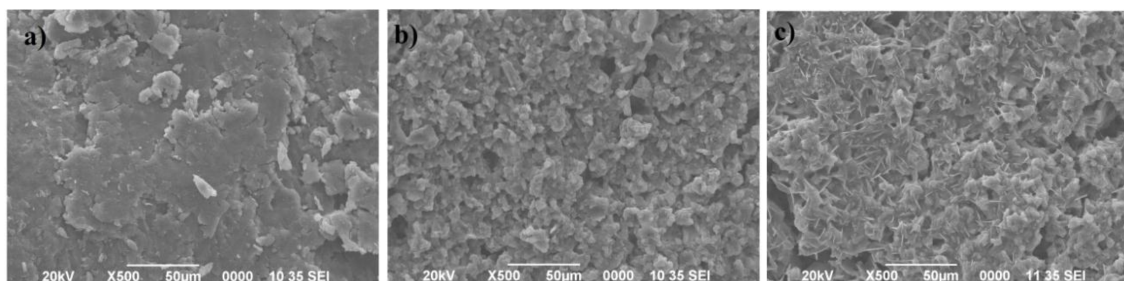


Figure 5.3. SEM images of (a) GO (b) GO/Gel/Glut and (c) GO/Gel/GST/Glut film.

### 5.4.2 Electrochemical impedance measurements

Electrochemical impedance spectroscopy (EIS) is an effective tool to characterize the biosensor by studying the interfacial properties of the modified electrode. Figure 5.4 shows the typical Nyquist plots obtained for bare Pt, Pt/GO/Gel, and Pt/GO/Gel/GST in 0.1 M KCl with equimolar (0.5 mM) $Fe(CN)_6^{3-/4-}$mixture, working frequency range 1 Hz to 7 MHz and at applied potential 0.30 V. Charge transfer resistance $R_{ct}$ found to be 27.29 Ω for bare Pt electrode (curve a), 164.20 Ω for Pt/GO/Gel modified electrode

(curve b) and 460.30 Ω for Pt/GO/Gel/GST modified electrode (curve c). As expected, $R_{ct}$ increased when Pt electrode was coated with GO-gelatin mixture. It increased further when GST was loaded. This increase in the $R_{ct}$ value is due to the fact that most biological molecules (including enzymes) are poor electrical conductors and hence cause hindrance to the electron transfer. This is the direct evidence of successful immobilization of GST on the electrode surface.

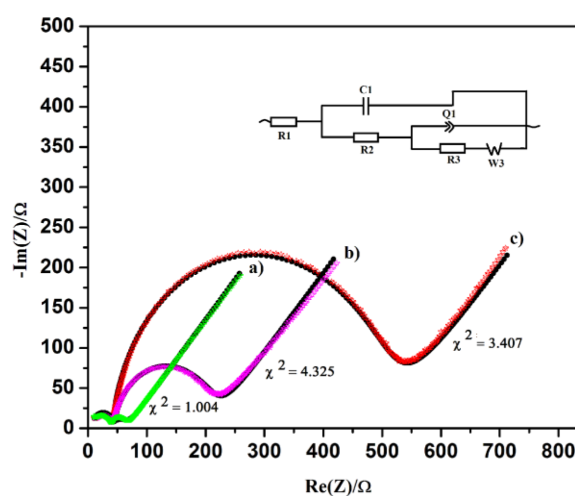


Figure 5.4. Nyquist plot of a) bare Pt b) Pt/GO/Gel and c) Pt/GO/Gel/GST in 0.1 M KCl containing 0.5 mM $K_3[Fe(CN)_6]$ and 0.5 mM $K_4[Fe(CN)_6]$. *Inset*: Best fit circuit model for evaluation of the parameters.

### 5.4.3 Cyclic voltammetric behaviour

Figure 5.5 shows the cyclic voltammetric behavior of the GSH-CDNB reaction with GST immobilized Pt working electrode in absence (curve 'a') and presence (curve 'b') of pesticides. The CV produces same oxidation peak (observed in case of unimmobilized enzyme) with peak maxima at 0.30 V (peak A, current 27.5 µA, RSD 3.33%) that gradually increases with successive CV runs and get stable after few runs, however, the peak current in this case is much more higher than the unimmobilized case. Another peak appeared from 0.60 V onwards (peak B, current 29.6 µA, RSD 1.66%). This peak is credited to methanol oxidation and the one at 0.30 V is attributed to oxidation of newly formed complex or intermediate. A low intensity oxidation peak C appeared at 0.05 V (RSD 3.84%) in the reverse cycle is attributed to oxidation of :COH produced through

dissociation of methanol. Low intensity reduction peak (D) appeared at 0.10 V (RSD 0.55%) is due to adsorption of $H_2$ at the platinum surface which normally shows up in the potential range from -0.23 to +0.20 V [22]. In presence of pesticides the intensity of peak A decreases (curve 'b').

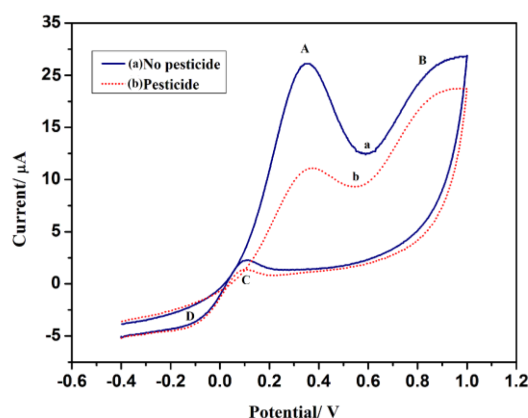


Figure 5.5. Cyclic Voltammograms recorded in a 1:1 volume mixture of 2 mM GSH in PB and 2 mM CDNB in 50% aqueous methanol in presence of modified Pt/GO/Gel/GST electrode at scan rate 20 mV/s. Curve 'a' was obtained before inhibition and 'b' after inhibition.

### 5.4.4 Chronoamperometric study

Inhibition was studied by two step procedure, measuring the chronoamperometric response before and after immersing the electrode (sensor) in pesticide solution. A typical chronoamperometric sensing response is shown in Figure 5.6. Curve 'a' is the initial response of the sensor to 2 mM GSH-CDNB solution and curve 'b' is the response after incubating the sensor in 50 ppb chlorpyrifos solution for 30 min. The Figure 5.6 clearly indicates that, as a result of inhibition, amperometric response of the biosensor decreases. During successive analysis the sensor was reactivated using PB solution.

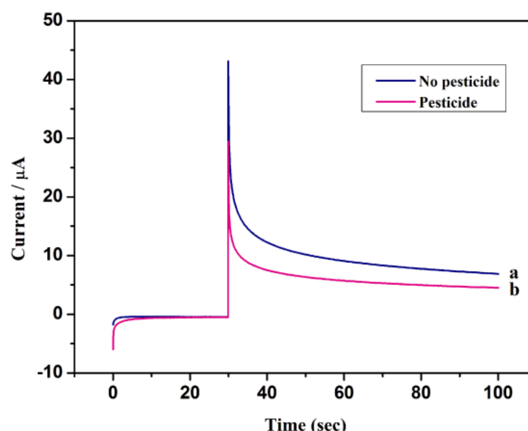


Figure 5.6. Chronoamperometric response of the biosensor towards GSH-CDNB solution a. in absence of inhibitor and b. in presence of inhibitor.

### 5.4.5 Sensor operational and kinetic parameters

Sensor operational parameters such as optimum pH, optimum inhibition time, intra and interstate precession, reusability and storage stability were determined.

Kinetic parameters such as apparent Michaelis-Menten constants, saturated substrate concentration and substrate specificity (between GSH and CDNB) and catalytic perfections of the reaction were evaluated.

#### 5.4.5.1 Saturated substrate concentration and apparent Michaelis-Menten constant

The saturated substrate concentration for both GSH and CDNB were determined through the Michaelis–Menten plot (Figure 5.7) measuring the variation of amperometric response with substrate concentration in CA mode. Concentration of one substrate was kept constant at 2 mM while varying the concentration of the other in the full range. The saturated substrate concentrations for both the substrates were found to be 4 mmol $L^{-1}$. The apparent Michaelis–Menten constant, $K_m^{app}$ was evaluated through the Lineweaver-Burk plot (Equation 5.1) and found to be 0.08 mmol $L^{-1}$ for GSH and 0.15 mmol $L^{-1}$ for CDNB. The observed value of GSH is lower than the previous study [18] in which the enzyme was in the free state. The $K_m^{app}$ value for CDNB found to be 0.15 mmol $L^{-1}$ which is almost similar to the one in unimmobilized state. Lowering of $K_m^{app}$ value of

GSH in the immobilized state indicates stronger binding of it with the enzyme in the immobilized state.

$$\frac{1}{i} = \frac{1}{i_{max}} + \frac{k_m^{app}}{i_{max}} \frac{1}{[S]} \qquad (5.1)$$

### 5.4.5.1.1 Substrate specificity

Stronger binding of GSH over CDNB is also obvious from the substrate specificity values. Determination of substrate specificity was done using assay developed by Habig *et al.* [23] and Simons *et al*. [24] as shown in "Appendix A(III)". Following equations were used to calculate substrate specificity values for both GSH and CDNB. Equation 5.2 based on Beer-Lambert law, was used to find the concentration of enzyme catalytic sites.

$$[ET] = (\Delta A \text{ x } 3 \text{ x } t') / 9.6 \text{ x } t \text{ x } 10^3 \qquad (5.2)$$

Here, t' is the time up to which the rate is determined and t is the time at which the reaction got almost completed. Numerical '3' represents the total volume of solution in the cuvette. The value 9.6 is millimolar extinction coefficient of Glutathione-1-Chloro-2,4-Dinitrobenzene conjugate at 340 nm. The value obtained for concentration of enzyme catalytic sites is 0.000039 mM and it is then followed by Equations 5.3 and 5.4 to determine turnover number or catalytic constant ($K_{cat}$) and catalytic efficiency (ε) of the enzyme.

$$K_{cat} = V_{max} / [ET] \qquad (5.3)$$

$$\varepsilon = K_{cat} / K_m \qquad (5.4)$$

$K_{cat}$ values for GSH and CDNB are 4658.97 $s^{-1}$ and 3215.38 $s^{-1}$ respectively. Substrate specificity was found to be $2.56 \times 10^7$ $s^{-1}M^{-1}$ and $2.15 \times 10^7$ $s^{-1}M^{-1}$ respectively for GSH and CDNB as substrates. The values indicate that GST has higher affinity for GSH than CDNB as substrate.

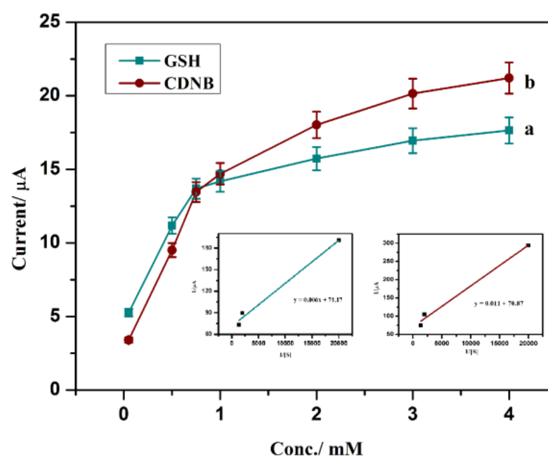


Figure 5.7. Dependency of peak current with substrate concentration. *Inset:* Lineweaver-Burk plot for determination of $K_m^{app}$ for both GSH and CDNB.

### 5.4.5.2 Effect of pH

The pH dependence of the enzyme electrode over the pH range 6.0-8.0 was studied through cyclic voltammetry. Figure 5.8 shows the cyclic voltammetric response of the sensor towards 2 mM GSH and CDNB at different solution pH. The maximum peak current was obtained at pH 8.0.

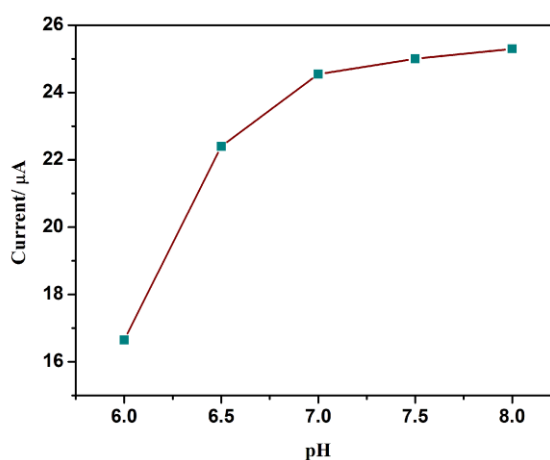


Figure 5.8. Effect of pH on the CV peak current of the sensor towards 2 mM GSH prepared in PB and 2 mM CDNB in 50% methanol when the enzyme loading was 20 µL and scan rate 20 mV/s.

### 5.4.5.3 Incubation time

The effect of inhibition time on the degree of inhibition was studied for the five pesticides taking a 100 ppb solution of each (Figure 5.9). Maximum inhibition time of each pesticide was found to be 30 min. The percentage inhibition of the biocatalyst was calculated using equation 5.5.

$$Inhibition(\%) = \frac{I_0 - I_i}{I_0} \times 100 \qquad (5.5)$$

Where, $I_0$ and $I_i$ are the CV peak currents obtained from the mixture before and after mixing pesticides.

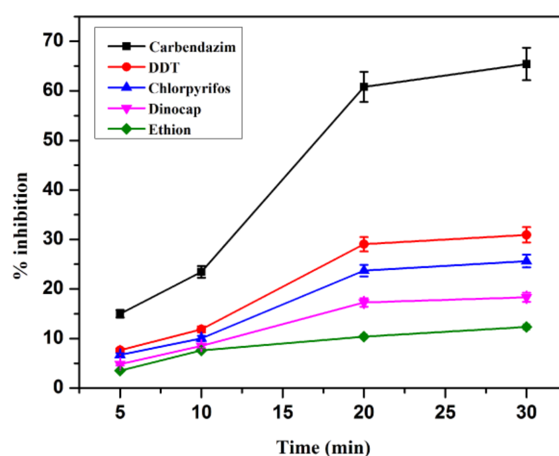


Figure 5.9. Variation of percent inhibition with incubation time determined from cyclic voltammetric response of the sensor towards 2 mM GSH prepared in PB and 2 mM CDNB in 50% methanol in presence of 100 μL of 100 ppb each of the pesticides.

### 5.4.5.4 Enzyme reactivation studies

For reactivation of the inhibited enzyme, the inhibited sensor was immersed in a solution of phosphate buffer (0.1 M) solution of pH 6.5 for 10 min. When the inhibition is less than 10%, 95-98% reactivation occurred. But when the percent inhibition is beyond 10%, reactivation efficiency decreased significantly. Reactivation efficiency was calculated by using equation 5.6 [16].

$$Reactivation\ (\%) = \frac{(I_a - I_s)}{(I_0 - I_s)} \times 100 \qquad (5.6)$$

Where, $I_0$ is the maximum peak current of the sensor in 2.0 mM each of GSH and CDNB, $I_s$ is the peak current after inhibition and $I_a$ is the same after reactivation.

#### 5.4.5.5 Enzyme leaching test

One of the main problems of biosensor use is leaching of enzyme from the electrode to the solution which affects the reproducibility of analysis. A successful immobilizing material should thus not only stabilize the enzyme, but also retain the enzyme from leaching into the test solution. Experiment was performed to check if any trace amount of enzyme can leach out from the immobilization matrix during electrochemical treatment of the sensor. This was done by performing several blank CV runs with the sensor, taking PB as the electrolyte followed by subjecting the same electrolyte to the assay procedure developed by Habig *et al*. [23] preparing CDNB in 50% methanol (the final methanol concentration in the assay was 25%). Absence of enzyme leakage was confirmed through the observation that no increase in UV absorption at 335 nm occurred as compared to the blank for a period of 30 min.

#### 5.4.5.6 Precision measurement

Inter-assay precision of the sensor was determined by measuring the CV response of six different fabrications when run in solution mixture comprised of 2 mM each of GSH and CDNB. The relative standard deviation (RSD) of the measurements was calculated. A value of 5.73% was obtained which indicates a good reproducibility of the fabrication process.

The intra state precision was determined by evaluating the RSD of sensor response for eight continuous CV runs with a single fabrication, using equimolar GSH-CDNB solution. The RSD was found to be 0.70%, which indicates that the sensor response has acceptable precision for consecutive measurements of GSH-CDNB reaction.

#### 5.4.5.7 Storage stability

To study the storage stability, a freshly prepared sensor after initial treatment kept at -20 $^0$C for 30 days. No significant loss in enzyme activity was found at the end of 30 days. We noticed that the stored sensor when subjected to continuous analysis at the end of the stored period (30 days) gave stable value up to 8-10 measurements.

### 5.4.6 Quantification of pesticides

CV method was used to quantify all the five pesticides. It was observed that when 50 ppb, 200 ppb, 150 ppb, 300 ppb and 400 ppb each of carbendazim, chlorpyrifos, DDT, dinocap and ethion respectively was mixed initially to six different solution mixtures and kept for 30 min, the CV peak at 0.30 V almost disappeared. Carbendazim, chlorpyrifos, DDT, dinocap and ethion solutions of concentration lower than aforementioned ones when mixed in separate reaction mixtures, found to suppress the peak current up to the extent proportional to the concentration. Based on this observation, calibration curves were obtained by plotting percentage inhibition versus pesticide concentration and were found to be linear. For determining the concentration based on peak current reduction, two solution mixtures containing GSH-CDNB-MeOH and PB of exactly same composition were prepared, one of which served as the blank. Triplicate measurements were made at each concentration of the five pesticides. Limit of detection is considered as the ppb of the pesticide required for 10% inhibition and found to be 2 ppb for carbendazim, 60 ppb for chlorpyrifos, 40 ppb for DDT, 50 ppb for dinocap and 100 ppb for ethion. The linear ranges for the five pesticides are found to be 2-50 ppb (y = 1.158x + 9.1113; $R^2$ =0.998) for carbendazim, 60-200 ppb (y = 0.492x -21.14; $R^2$ = 0.998) for chlorpyrifos, 40-150 ppb (y = 0.412x – 2.810; $R^2$ =0.989) for DDT, 50-300 ppb (y = 0.248 x – 8.577; $R^2$ =0.999) for dinocap and 100-400 ppb (y = 0.154x - 6.598; $R^2$ = 0.995) for ethion. Figure 5.10 shows the various calibration curves.

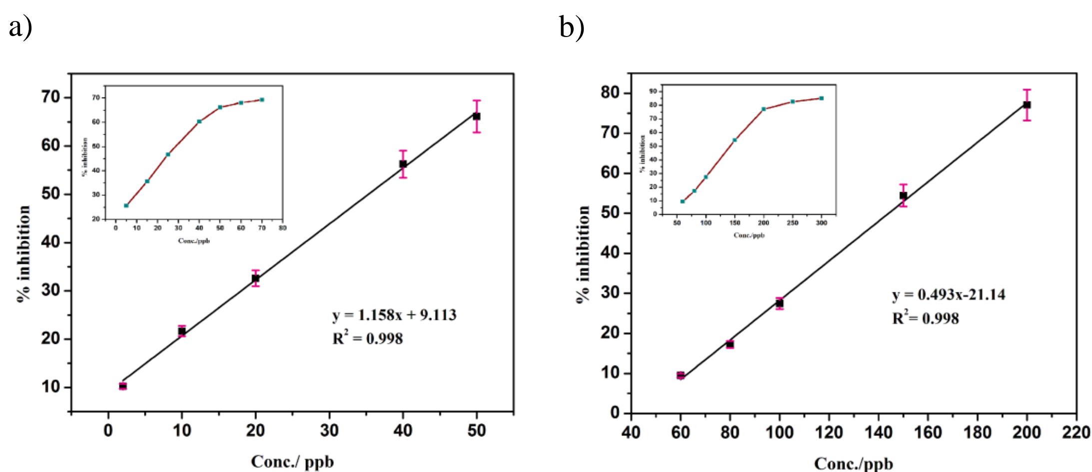

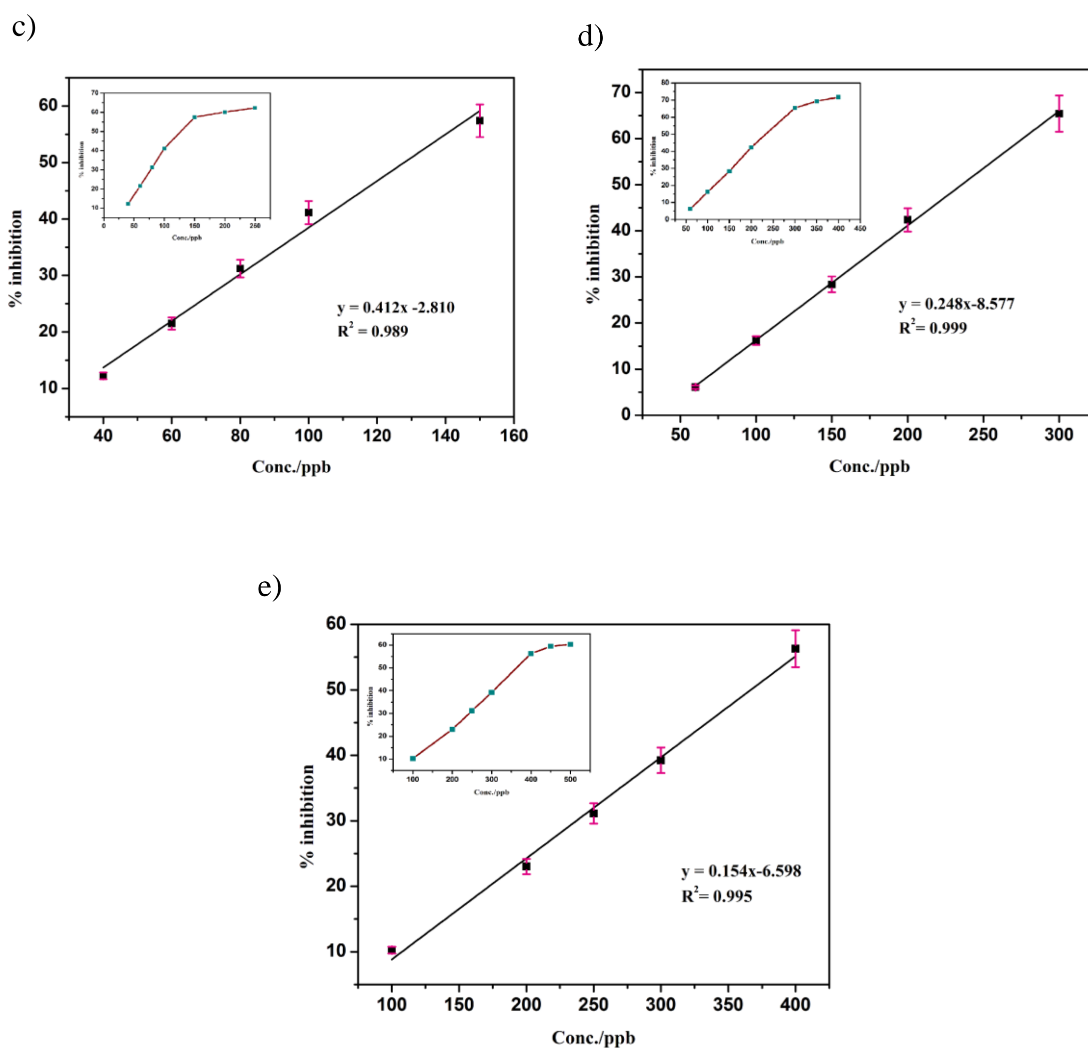


Figure 5.10. Calibration curves for a) carbendazim b) chlorpyrifos c) DDT d) dinocap and e) ethion.

A comparison of the performance of the present biosensor with few other biosensors reported in literature is shown in table 5.1.

Table 5.1. Comparison of the performance of the present biosensor with other biosensors when applied to the same pesticide.

| Pesticide | Method of detection | Limit of detction | Linear range | Ref. |
|---|---|---|---|---|
| Carbendazim | DNA Aptamer based biosensor immobilized on gold surface | 0.0082 ppb | 0.01 ppb - 10 ppb | [25] |

| | | | | |
|---|---|---|---|---|
| | GST biosensor using graphene oxide | 2 ppb | 2-50 ppb | This work |
| Chlorpyrifos | Acetylcholinesterase (AChE) immobilized on Fc-F hydrogel support | 1.00 ppb | 1.75-263 ppb | [26] |
| | GST biosensor using graphene oxide | 60 ppb | 60-200 ppb | This work |
| DDT | Surface plasmon resonance (SPR) based immunosensor | 0.015 ppb | Not reported | [27] |
| | Gold nanoparticles (GNPs) based immunoassay | 27 ppb | 27 -1000 ppb | [28] |
| | GST biosensor using graphene oxide | 40 ppb | 40-150 ppb | This work |
| Dinocap | GST biosensor using graphene oxide | 50 ppb | 50-300 ppb | This work |
| | No other biosensing method reported so far. | - | - | - |
| Ethion | Butyrylcholinesterase biosensor based on multi-walled carbon nanotube–polyvinyl chloride (MWNT–PVC) composite | 22 ppb | 22- 330 ppb | [29] |
| | GST biosensor using graphene oxide | 100 ppb | 100-400 ppb | This work |

### 5.4.7 Validation study

Biosensor results were validated by performing a two-step validation experiment. In the first step the recovery of the applied sample pre-treatment process was determined by preparing a GC calibration curve for the pesticide, taking solutions of analytical standard sample of ethion. Then the recovery from spiked potato samples were determined. In the second step, the same fortified solution extract was subjected to bioanalysis and the results were compared with recovery values obtained through GC analysis. The concentration range for the GC calibration curve was from 100 ppb to 1000 ppb and the analytical solution for both GC and bioanalysis was prepared by fortifying potato samples with 300 ppb of ethion. The stepwise solid phase extraction procedure is as follows: chopped vegetable (potato) weighing 10 grams was spiked with 5 mL of 300 ppb ethion solution (prepared in acetonitrile) and then homogenized. Then, 5 mL of acetonitrile was added and shaken in a vortex shaker for 5 minutes, followed by sonication for 5 minutes and then centrifuged for 10 minutes at 2000 rpm. Then the supernatant was separated out and passed through a pre-conditioned (acetonitrile–hexane mixture in a 3:1 ratio) column of size 14 mm x 160 mm and packed with 5 g each of bondesil-$NH_2$ and carbon SPE bulk sorbent. The solution passing out through the column was collected in a 50 mL round-bottom flask and evaporated to dryness at 40 $^0$C and 200 mbar in a rotary evaporator. The dry residue was reconstituted in a mixture of 4 mL methanol and 1 mL dichloromethane and evaporated again to about 1 mL and then diluted to 5 mL by adding more methanol solution. To 1 mL of this solution, 1 mL each of 2 mM GSH and CDNB, and 20 µL of GST was added. The percentage of inhibition in peak current was calculated and the amount of pesticide was determined with the help of the calibration curve and considering the dilution factor. The entire process was repeated thrice to get triplicate results.

Recovery for ethion from potato samples was found to be 88.2% (RSD = 4.6%, n = 5) in the GC analysis and, 88.6% (RSD = 5.8%., n = 5) in bioanalysis using the fabricated biosensor probe. Close resemblance of the bioanalysis results with the GC results infers that the bioanalysis method is perfect and highly reliable. The gas chromatograms of ethion under the specified analytical parameters are shown in figure 5.11a and 5.11b.

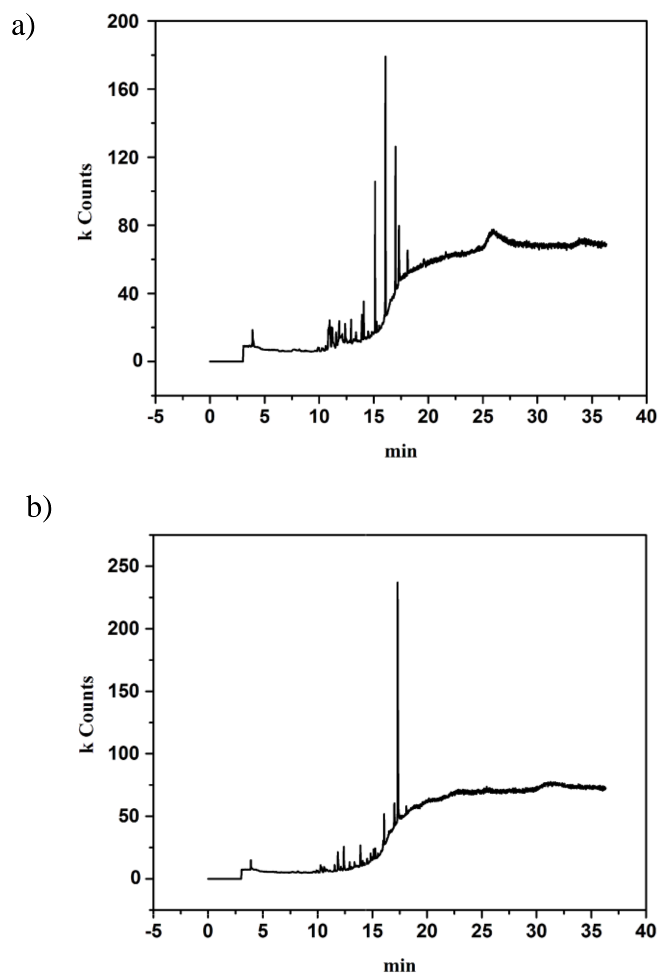


Figure 5.11 a) Gas chromatogram of 400 ppb ethion and b) 1000 ppb ethion.

## 5.5 Conclusion

We have shown for the first time that the enzyme GST can be immobilized on platinum electrode using graphene oxide and gelatin matrix to fabricate an enzyme electrode that can act as sensor probe with broad spectrum applicability. The sensor can be applied to detect amperometrically different classes of pesticides. The reproducibility of sensor results was confirmed through GC analysis. We have also reported for the first time the catalytic perfection as well as substrate specificity of the enzyme GST towards the two substrates CDNB and GSH.

## References

[1] Zdarta, J., Meyer, A. S., Jesionowski, T., and Pinelo, M. A general overview of support materials for enzyme immobilization: Characteristics, properties, practical utility. *Catalysts*, 8(2):92, 2018.

[2] Dutta, R. R. and Puzari, P. Amperometric biosensing of organophosphate and organocarbamate pesticides utilizing polypyrrole entrapped acetylcholinesterase electrode. *Biosensors and Bioelectronics*, 52:166-172, 2014.

[3] Soylemez, S., Kanik, F. E., Ileri, M., Hacioglu, S. O., and Toppare, L. Development of a novel biosensor based on a conducting polymer. *Talanta*, 118:84-89, 2014.

[4] Cesarino, I., Moraes, F. C., Lanza, M. R. V., and Machado, S. A. S. Electrochemical detection of carbamate pesticides in fruit and vegetables with a biosensor based on acetylcholinesterase immobilised on a composite of polyaniline–carbon nanotubes. *Food Chemistry*, 135(3):873-879, 2012.

[5] Viswanathan, S., Radecka, H., and Radecki, J. Electrochemical biosensor for pesticides based on acetylcholinesterase immobilized on polyaniline deposited on vertically assembled carbon nanotubes wrapped with ssDNA. *Biosensors and Bioelectronics*, 24(9):2772-2777, 2009.

[6] Kuila, T., Bose, S., Khanra, P., Mishra, A.K., Kim, N.H., and Lee, J.H. Recent advances in graphene-based biosensors. *Biosensors and Bioelectronics,* 26:4637-4648, 2011.

[7] Li, Y., Shi, L., Han, G., Xiao, Y., and Zhou, W. Electrochemical biosensing of carbaryl based on acetylcholinesterase immobilized onto electrochemically inducing porous graphene oxide network. *Sensors and Actuators B: Chemical,* 238:945-953, 2017.

[8] Raghu, P., Swamy, B. E. K., Reddy, T. M., Chandrashekar, B. N., and Reddaiah, K. Sol–gel immobilized biosensor for the detection of organophosphorous pesticides: a voltammetric method. *Bioelectrochemistry*, 83:19-24, 2012.

[9] Raghu, P., Reddy, T. M., Reddaiah, K., Swamy, B. E. K., and Sreedhar, M. Acetylcholinesterase based biosensor for monitoring of malathion and acephate in food samples: a voltammetric study. *Food chemistry*, 142:188-196, 2014.

[10] Tcheumi, H. L., Tonle, I. K., Ngameni, E., and Walcarius, A. Electrochemical analysis of methylparathion pesticide by a gemini surfactant-intercalated clay-modified electrode. *Talanta*, 81(3):972-979, 2010.

[11] Gong, A., Zhu, C. T., Xu, Y., Wang, F. Q., Tsabing, D. K., Wu, F. A., and Wang, J. Moving and unsinkable graphene sheets immobilized enzyme for microfluidic biocatalysis. *Scientific Reports*, 7(1):4309, 2017.

[12] Yang, Y., Asiri, A. M., Du, D., and Lin, Y. Acetylcholinesterase biosensor based on a gold nanoparticle–polypyrrole–reduced graphene oxide nanocomposite modified electrode for the amperometric detection of organophosphorus pesticides. *Analyst*, 139(12):3055-3060, 2014.

[13] Cui, H. F., Wu, W. W., Li, M. M., Song, X., Lv, Y., and Zhang, T. T. A highly stable acetylcholinesterase biosensor based on chitosan-$TiO_2$-graphene nanocomposites for detection of organophosphate pesticides. *Biosensors and Bioelectronics*, 99:223-229, 2018.

[14] Wang, Y., Zhang, S., Du, D., Shao, Y., Li, Z., Wang, J., Engelhard, M. H., Li, J., and Lin, Y. Self assembly of acetylcholinesterase on a gold nanoparticles–graphene nanosheet hybrid for organophosphate pesticide detection using polyelectrolyte as a linker. *Journal of Materials Chemistry*, 21(14):5319-5325, 2011.

[15] Zhao, H., Ji, X., Wang, B., Wang, N., Li, X., Ni, R., and Ren, J. An ultra-sensitive acetylcholinesterase biosensor based on reduced graphene oxide-Au nanoparticles-β-cyclodextrin/Prussian blue-chitosan nanocomposites for organophosphorus pesticides detection. *Biosensors and Bioelectronics*, 65:23-30, 2015.

[16] Zhang, J., Zhang, F., Yang, H., Huang, X., Liu, H., Zhang, J., and Guo, S. Graphene oxide as a matrix for enzyme immobilization. *Langmuir*, 26(9):6083-6085, 2010.

[17] Yu, J., Yu, D., Zhao, T., and Zeng, B. Development of amperometric glucose biosensor through immobilizing enzyme in a Pt nanoparticles/mesoporous carbon matrix. *Talanta*, 74(5):1586-1591, 2008.

[18] Borah, H., Dutta, R. R., Gogoi, S., and Puzari, P. Influence of methanol, ethanol and cypermethrin on the Glutathione S-tranferase catalyzed reaction of Glutathione with 1-chloro-2,4-dinitrobenzene: A method for detection and quantification of cypermethrin. *Electrochimica Acta*, 205:198-206, 2016.

[19] Borah, H., Dutta, R. R., Gogoi, S., Medhi, T., and Puzari, P. Glutathione-S-transferase-catalyzed reaction of glutathione for electrochemical biosensing of temephos, fenobucarb and dimethoate. *Analytical Methods*, 9(27):4044-4051, 2017.

[20] Paulchamy, B., Arthi, G., and Lignesh, B. D. A simple approach to stepwise synthesis of graphene oxide nanomaterial. *Journal of Nanomedicine and Nanotechnology*, 6(1):1, 2015.

[21] Li, Z., Kinloch, I. A., and Young, R. J. The role of interlayer adhesion in graphene oxide upon its reinforcement of nanocomposites. *Philosophical Transactions of the Royal Society A*, 374(2071):20150283, 2016.

[22] Zhou, C., Wang, H., Peng, F., Liang, J., Yu, H., and Yang, J. $MnO_2$/CNT supported Pt and PtRu nanocatalysts for direct methanol fuel cells. *Langmuir*, 25(13):7711-7717, 2009.

[23] Habig, W. H., Pabst, M. J., and Jakoby, W. B. Glutathione S-transferases the first enzymatic step in mercapturic acid formation. *Journal of Biological Chemistry*, 249(22):7130-7139, 1974.

[24] Simons, P. C. and Vander Jagt, D. L. Purification of Glutathione S-Transferases from Human Liver by Glutathione-Affinity Chromatography. *Analytical Biochemistry*, 82(2):334-349, 1977.

[25] Eissa, S. and Zourob, M. Selection and characterization of DNA aptamers for electrochemical biosensing of carbendazim. *Analytical Chemistry*, 89(5):3138-3145, 2017.

[26] Xia, N., Zhang, Y., Chang, K., Gai, X., Jing, Y., Li, S., Liu, L., and Qu, G. Ferrocene-phenylalanine hydrogels for immobilization of acetylcholinesterase and detection of chlorpyrifos. *Journal of Electroanalytical Chemistry*, 746:68-74, 2015.

[27] Mauriz, E., Calle, A., Manclus, J. J., Montoya, A., Hildebrandt, A., Barceló, D., and Lechuga, L. M. Optical immunosensor for fast and sensitive detection of DDT and related compounds in river water samples. *Biosensors and Bioelectronics*, 22(7):1410-1418, 2007.

[28] Lisa, M., Chouhan, R. S., Vinayaka, A. C., Manonmani, H. K., and Thakur, M. S. Gold nanoparticles based dipstick immunoassay for the rapid detection of dichlorodiphenyltrichloroethane: An organochlorine pesticide. *Biosensors and Bioelectronics*, 25(1):224-227, 2009.

[29] Khaled, E., Kamel, M. S., Hassan, H. N. A., Abdel-Gawad, H., and Aboul-Enein, H. Y. Performance of a portable biosensor for the analysis of ethion residues. *Talanta*, 119:467-472, 2014.